ELSEVIER

0267-7261(95)00049-6

Soil Dynamics and Earthquake Engineering 15 (1996) 233–244

0267-7261/96/$15.00

Nonlinear analysis for dynamic lateral pile response

M. H. El Naggar & M. Novak†

Department of Civil Engineering, The University of Western Ontario, London, Ontario, Canada, N6A 5B9

(Received 3 June 1994; revised version received 27 November 1995; accepted 27 November 1995)

An analysis of pile lateral response to transient dynamic loading and to harmonic loading is presented allowing for nonlinear soil behavior, discontinuity conditions at the pile–soil interface and energy dissipation through different types of damping. Furthermore, the effect of neighbouring piles is taken into account for piles in a group. The validity of the approach was examined and a reasonable agreement with field tests and more rigorous solutions was found. Equivalent linear stiffness and damping parameters of single piles and interaction factors for approximate nonlinear analysis are presented. Copyright © 1996 Elsevier Science Limited.

Key words: pile dynamics, lateral response, nonlinear, pile interaction, transient response.

INTRODUCTION

Piles are frequently subjected to lateral forces that result from loading on supported structures such as building, quay walls and offshore structures.

Various approaches have been developed for the static and dynamic lateral response of piles such as finite element analysis,[1,2] but this approach requires large computational efforts. The boundary element approach is also used,[3,4] but the inclusion of the soil nonlinear behavior in this approach is difficult. The Winkler model, although approximate, seems to be a powerful technique to model the response of single piles and pile groups to lateral dynamic loads. Matlock *et al.*[5] developed a unit load transfer curves approach, also known as *p-y* curves, for the time domain nonlinear analysis. Nogami & Konagai[6] have developed a time domain analysis method for flexural response of single piles based on the frequency domain solution developed by Novak *et al.*[7] Nogami *et al.*[17] accounted for the soil nonlinearity by introducing a multi-linear element for the inner field, and a gap element with a pre-estimated factor to account for plastic deformations and gap opening at the pile–soil interface. They also accounted for the group effect and the wave propagation away from the pile by introducing a far field element of three units in series, each has a spring and dashpot.

In this study, a computationally efficient model for lateral response of single piles and pile groups is developed. The model developed accounts for the nonlinear behavior of the soil adjacent to the pile, and slippage and gapping at the soil–pile interface in a rational manner. The energy dissipation in the soil through different types of damping is also included in the analysis. For the most part, the parameters of the model are standard geotechnical parameters.

SINGLE PILE MODEL

The piles are assumed to be vertical with a circular cross-section embedded in a horizontally nonlinear layered soil. Based on the Winkler hypothesis, the soil is divided into a number of layers. Piles are also divided into segments with the same number and length as the soil layers. The analysis is formulated in the time domain to facilitate the modeling of the nonlinear behavior and discontinuity conditions. The elements of this model are shown in Fig. 1 and are discussed in detail in the following sections.

Soil reactions modeling

In each layer the soil model is divided into two parts as shown in Fig. 1. The first part is an inner field model to which nonlinearity is confined. The second part is a far field model which accounts for wave propagation away from the pile. In this model, the soil reactions at both sides of the pile are modeled separately to account for the

† Deceased.

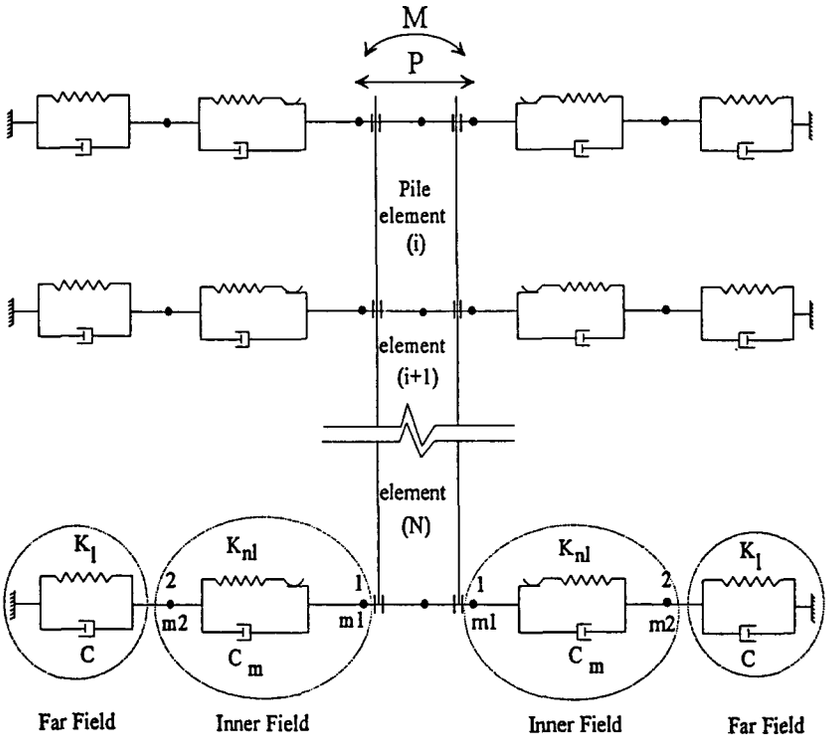

Fig. 1. Elements of the proposed model for nonlinear dynamic analysis of lateral response of single piles.

state of stress and discontinuity conditions at both sides as the load direction changes.

Inner field element. The soil reaction of the inner field is modeled by a nonlinear spring the stiffness of which is calculated with the assumption that plane stress conditions hold, the inner field is a homogeneous isotropic viscoelastic medium, the pile is rigid and circular, there is no separation at the soil–pile interface, and the displacements are small. The stiffness solution under these conditions was obtained by Noval & Sheta[8] as

$$k_{nl} = \frac{8\pi G_m(1-\nu)(3-4\nu)[(r_0/r_1)^2+1]}{(r_0/r_1)^2+(3-4\nu)^2[(r_0/r_1)^2+1]\ln(r_1/r_0)-1}, \quad (1)$$

where r_0 and r_1 are the inner and outer radii of the inner field, respectively, and ν is the Poisson's ratio of the soil stratum. G_m is the modified shear modulus calculated according to the strain level, assuming that Poisson's ratio is constant, as

$$G_m = G_{max}(1-\eta) \quad (2)$$

G_{max} is the initial shear modulus of the soil layer, η is the mobilization ratio defined as $\eta = P/P_U$, where P is the horizontal load at the spring and P_U is the ultimate resistance of the spring calculated using the standard relations given by the API.[9] For clay, the resistance is given as a strength per unit length of the soil layer by

$$P_U = 3c_u d + \gamma X d + J c_u X \quad X \leqslant X_R \quad (3)$$

$$P_U = 9c_u d \quad X > X_R, \quad (4)$$

where c_u = undrained shear strength, hd = pile diameter, γ is the effective unit weight of soil, J = empirical coefficient ranging from 0·25 to 0·5, X = depth below the surface and X_R = depth of the reduced resistance zone, which can be calculated by solving eqns (3) and (4) simultaneously.

The corresponding criteria for the lateral resistance of sands at shallow depths P_{U1} or at large depth P_{U2} are

$$P_{U1} = A\left\{\gamma X\left[\frac{K_0 X\tan\phi\sin\beta}{\tan(\beta-\phi)\cos\alpha} + \frac{\tan\beta}{\tan(\beta-\phi)}(d + X\tan\beta\tan\alpha) + K_0 X\tan\beta(\tan\phi\sin\beta-\tan\alpha) - K_a d\right]\right\} \quad (5)$$

$$P_{U2} = A\gamma X d[K_a(\tan^8\beta - 1) + K_0\tan\phi\tan^4\beta]. \quad (6)$$

In these equations, A is an empirical adjustment factor dependent on the depth from the soil surface and can be found in Ref. 9, K_0 is the earth pressure coefficient at rest (0·4), ϕ is the effective friction angle of the sand, $\beta = \phi/2 + 45°$, $\alpha = \phi/2$, K_a is the Rankin minimum active earth pressure coefficient defined as $K_a = \tan^2(45° - \phi/2)$.

Far field element. Novak *et al.*[7] solved the problem of the horizontal vibration of piles. In their solution, the plane strain conditions are assumed to hold. An explicit solution for the soil horizontal complex stiffness of a unit length of a cylinder embedded in a linear viscoelastic

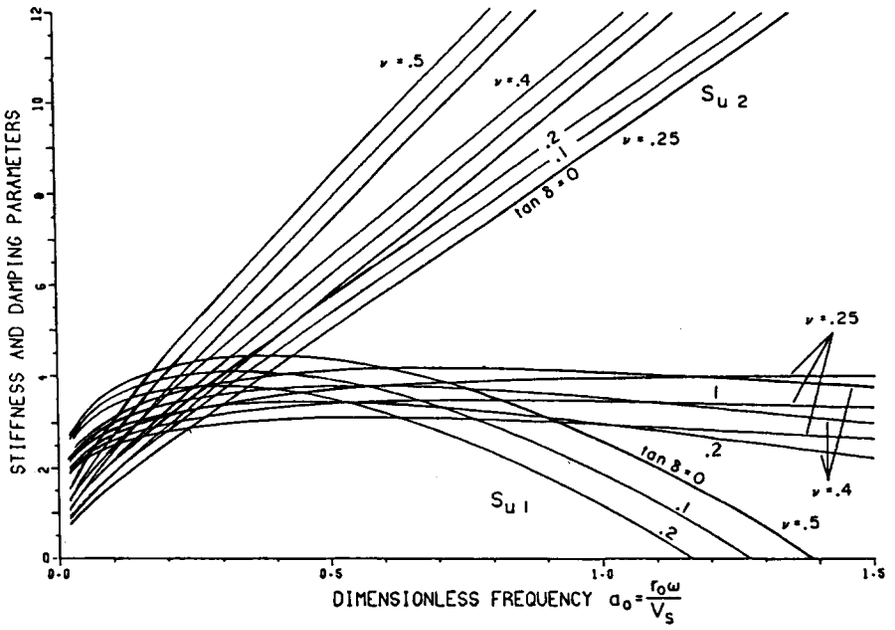

Fig. 2. Variations of horizontal stiffness and damping parameters, S_{u1} and S_{u2}, with dimensionless frequency a_0 and soil Poisson's ratio (after Novak *et al.*[7]).

medium is given by

$$K = \pi G a_0^2 T. \tag{7}$$

In this equation $G = G_{max}$ is the initial shear modulus of the soil layer, $a_0 = \omega r_0 / V_s$ is a dimensionless frequency and T is a dimensionless factor given by

$$T = -\frac{4K_1(b_0^*)K_1(a_0^*) + a_0^* K_1(b_0^*)K_0(a_0^*) + b_0^* K_0(b_0^*)K_1(a_0^*)}{b_0^* K_0(b_0^*)K_1(a_0^*) + a_0^* K_1(b_0^*)K_0(a_0^*) + b_0^* a_0^* K_0(b_0^*)K_0(a_0^*)}, \tag{8}$$

where a_0^* and b_0^* are complex dimensionless frequencies defined as

$$a_0^* = \frac{ia_0}{\sqrt{1+iD_s}}, \qquad b_0^* = \frac{ia_0}{\xi\sqrt{1+iD_l}} \tag{9}$$

in which ξ is the ratio between the longitudinal and shear wave velocities of the soil layer, D_s and D_l are the material damping constants, usually assumed to be both equal to D, associated with shear and longitudinal waves, respectively, and finally, K_0 and K_1 are the modified Bessel functions of the second kind of orders 0 and 1, respectively. This solution is not suitable for the time domain analysis because it is frequency dependent. However, the real and imaginary parts may be separated and eqn (7) can be rewritten as

$$K + G[S_{u1}(a_0, \nu, D) + iS_{u2}(a_0, \nu, D)] \tag{10}$$

in which S_{u1} and S_{u2} are real. Figure 2 shows the variations of S_{u1} and S_{u2} with the dimensionless frequency a_0 and ν. It may be observed from the figure that for the frequency range between 0·05 and 0·5, typical of offshore loading and many other applications, S_{u1} may be considered constant, while S_{u2} increases monotonically with a_0. The effect of Poisson's ratio is that as it increases, both of S_{u1} and S_{u2} increase in the specified range of frequency. These observations suggest that the outer field element can be modeled by a spring and dashpot whose constants depend on Poisson's ratio, but they are frequency independent and defined as

$$\begin{aligned} K_1 &= GS_{u1}(\nu) \\ c &= \frac{cGr_0}{V_s} S_{u2}(a_0 = 0{\cdot}5, \nu), \end{aligned} \tag{11}$$

where S_{u1} and S_{u2} are frequency independent with their values chosen according to Poisson's ratio of the soil layer and the dominant dimensionless frequency a_0. These frequency independent stiffness and damping parameters are used in the dynamic analysis in the time domain.

Discontinuity conditions. Discontinuity conditions of the motion between pile and soil are caused by the slippage and gapping at the soil–pile interface. To model these conditions logically the soil reactions to the pile motion at both sides are modeled separately as shown in Fig. 1. The load–deflection curve for a pile node at the topmost part of the pile, where soil–pile separation takes place, is shown in Fig. 3 as well as the corresponding horizontal displacements of the soil nodes on both sides of the pile. For the pile initially loaded rightward, the soil node at the left is separated from the pile as the force in the near field element reaches zero, assuming that soil does not resist tension. The soil node on the right is pushed with the pile to the right and K_{nl} decreases as the load increases. In the unloading phase

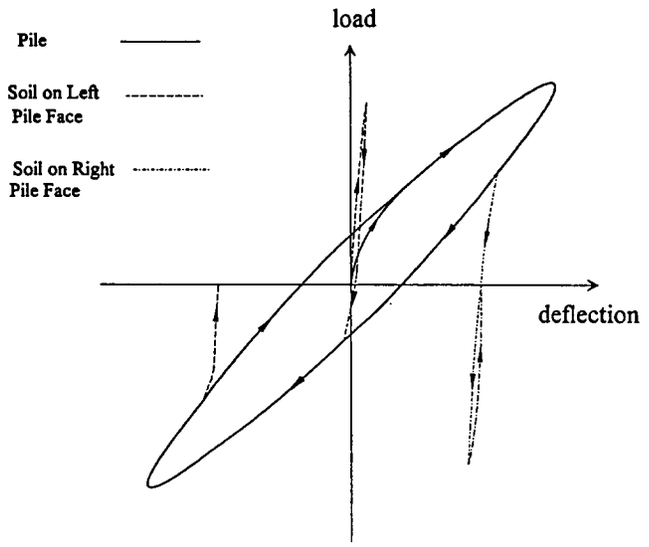

Fig. 3. Pile and soil displacements for a case with pile–soil separation.

the pile separates from the soil on its right also. When the pile is loaded more leftward, it comes into contact again with the soil node on its left and pushes it until unloading occurs again, separation takes place and the pile returns to its original position. The result of this is that the soil nodes are left in a displaced position and a permanent gap develops. The development of such gaps is a phenomenon observed in offshore piles especially after storm conditions, however, afterward healing occurs and the gaps are closed. Development of these gaps greatly affects the pile response to any subsequent loading as will be discussed later.

Pile modeling

The pile shaft is assumed to be elastic, vertical and has a circular cross-section. It is subdivided into a number of elements and every element is assumed to have a constant cross-reaction. The structural stiffness matrix of each individual element is defined by the standard four by four bending stiffness matrix relating the translation u and rotation θ to load P and moment M and is given as

$$E_p I_p \begin{bmatrix} 12/l^3 & -12/l^3 & 6/l^2 & 6/l^2 \\ -12/l^3 & 12/l^3 & -6/l^2 & -6/l^2 \\ 6/l^2 & -6/l^2 & 4/l & 2/l \\ 6/l^2 & -6/l^2 & 2/l & 4/l \end{bmatrix} \begin{Bmatrix} u_1 \\ u_2 \\ \theta_1 \\ \theta_2 \end{Bmatrix} = \begin{Bmatrix} P_1 \\ P_2 \\ M_1 \\ M_2 \end{Bmatrix}, \quad (12)$$

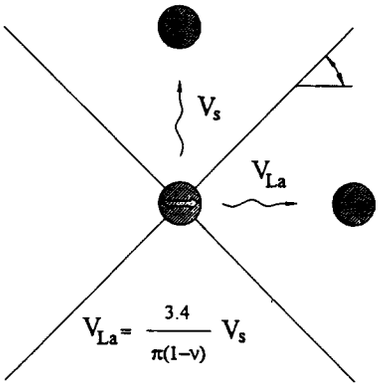

Fig. 4. Assumed apparent velocities of waves emanating from a laterally oscillating pile (after Gazetas & Dobry[13]).

where E_p and I_p are Young's modulus and second moment of area of the pile, respectively, and l is the element length. The pile structural stiffness matrix may then be constructed by superposition of the sub-matrices of the individual elements.

The number of elements has a great effect on the accuracy of the results. Poulos[10] found that the greater the number of the elements the greater the accuracy of the results. El Sharnouby & Novak[11] found that using 12 pile elements increasing in length with depth, with the top elements 1/4 of the average element length gave accurate results with a minimum of computational efforts. However, for dynamic analysis it is somewhat different. A sensitivity study was done and 20 elements increasing in length with depth were found to give accurate results.

To reduce the computational efforts, only degrees of freedom of interest are maintained and the rest are eliminated through a static condensation process. Thus, only the transitional degrees of freedom along the pile and the rotational degree of freedom at the pile head are maintained.

GROUP EFFECT

Since each pile is affected not only by its own load, but also by the load and deflection of other piles in the group, the dynamic stiffness of a group of piles is greatly affected by the interaction between piles. This effect is incorporated in the analysis as follows. For the lateral vibration, interaction between piles depends on the angle, θ, between the lines of the two piles and the direction of the horizontal applied force, as well as the spacing between them. Gazetas & Dobry[13] found that the 90^0-passive pile m (Fig. 4) is affected essentially only by S-waves which emanate from active pile 1 and which have a phase velocity V_s. They also found that the 0^0-passive pile is affected by compression–extension waves coming from the active pile and propagating with an apparent phase velocity which is equal to the so-called

Lysmer's analog velocity V_{La} given by

$$V_{La} = \frac{3{\cdot}4V_s}{\pi(1-\nu)}. \tag{13}$$

Assuming that waves propagate in the horizontal direction only and also assuming a Winkler soil model, the displacement at any point in the elastic soil domain may be given (Makris & Gazetas[14]), in general, as

$$u(a_0, r, \theta) = u_0 \psi_u(a_0, r, \theta) \tag{14}$$

In eqn (14) u_0 is the amplitude of the disturbance at the source, and ψ_u is an attenuation function accounting for the wave propagation away from the source and the radiation damping. It is sufficient to compute ψ_u only for $\theta = 0^0$ and $\theta = 90^0$ and the approximation by Dobry & Gazetas[18] may be used to evaluate ψ_u at any angle θ as

$$\psi_u(a_0, r, \theta) = \psi_u(a_0, r, 0^0)\cos^2\theta + \psi_u(a_0, r, 90^0)\sin^2\theta \tag{15}$$

in which

$$\psi_u(a_0, r, 0^0) = \sqrt{\frac{r_0}{r}}\, e^{-ia_0\frac{\pi(1-\nu)(r-r_0)}{3{\cdot}4r_0}}$$
$$\psi_u(a_0, r, 90^0) = \sqrt{\frac{r_0}{r}}\, e^{-ia_0\frac{(r-r_0)}{r_0}}. \tag{16}$$

Using this approximation for the attenuation function, eqn (14) may be rewritten as

$$u(a_0, r, 0^0) = \frac{1}{K_1 + ica_0}\sqrt{\frac{r_0}{r}}\, e^{-ia_0\frac{\pi(1-\nu)(r-r_0)}{3{\cdot}4r_0}} P_h(a_0)$$
$$u(a_0, r, 90^0) = \frac{1}{K_1 + ica_0}\sqrt{\frac{r_0}{r}} e^{-ia_0\frac{(r-r_0)}{r_0}} P_h(a_0), \tag{17}$$

where K_1 and c are the frequency independent spring and dashpot constants defined in eqn (11). Subjecting eqn (17) to an inverse Fourier transform, the unit impulse response function required for time domain analysis is obtained as

$$u(t, r) = \sqrt{\frac{r_0}{r}} A\, e^{-B(t-t_0)} \quad t > t_0 \tag{18}$$

where $A = 1/c$, $B = K_1/c$ and t_0 is given by

$$t_0 = \frac{\pi(1-\nu)(r-r_0)}{3{\cdot}4V_s} \quad \theta = 0^0$$
$$t_0 = \frac{(r-r_0)}{V_s} \quad \theta = 90^0. \tag{19}$$

The interaction effect is assumed to vary linearly through each time step Δt. The soil displacement at the axis of the mth pile due to a disturbance at the lth pile is given by

$$u_m(t_i, r_{ml}) = P_l(t_i - t_{ml-1})H_1(t_i, r_{ml}) + P_l(t_i)H_2(t_i, r_{ml}), \tag{20}$$

where i is the number of the time step, r_{ml} is the distance between the piles m and l, t_{ml-1} is the travel time between them minus one time step; H_1 and H_2 are convolution integrals over the period Δt given as

$$H_1 = \int_0^{\Delta t} u(t-\tau, r)\left(1 - \frac{\tau}{\Delta T}\right)d\tau$$
$$= \sqrt{\frac{r_0}{r}}\frac{A}{B}\left[\frac{1}{B\Delta t}e^{B\Delta t} - \left(1 - \frac{1}{B\Delta t}\right)\right]e^{-B(t-t_0)}$$
$$t \geqslant t_0 + \Delta t \tag{21}$$

$$H_2 = \int_0^{\Delta t} u(t-\tau, r)\frac{\tau}{\Delta T}d\tau$$
$$= \sqrt{\frac{r_0}{r}}\frac{A}{B}\left[\left(1 - \frac{1}{B\Delta t}\right)e^{B\Delta t} + \frac{1}{B\Delta t}\right]e^{-B(t-t_0)}$$
$$t \geqslant t_0 + \Delta t. \tag{22}$$

Equation (20) implies that H_2 is the inverse of the time domain stiffness of the medium if r equals to r_0, yielding the interaction force as

$$P = -[H_2(r = r_0)]^{-1}u_m \quad l \neq m$$
$$= -K_u u_m. \tag{23}$$

For $\theta = 0^0$ or 90^0 relevant values of t_0 from eqn (19) are to be substituted in eqns (21) and (22). For any value of θ eqn (15) can be used to obtain the interaction force, P. This force is to be considered in the analysis as discussed in the subsequent section.

Figure 5 shows a slice of the soil–pile system containing the elements of the model implemented in the group analysis. The visco-elastic spring, K_u, connects the two piles through the far field.

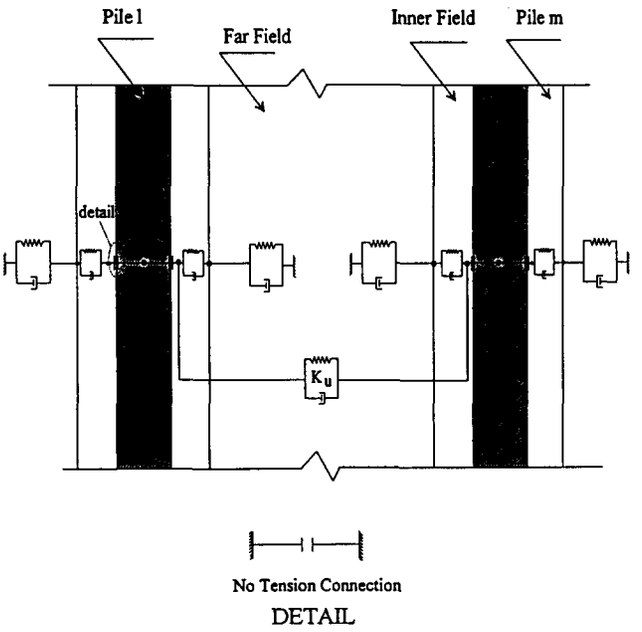

Fig. 5. Elements of the model implemented in the nonlinear analysis of lateral response of pile group.

EQUATIONS OF MOTION

The mass of the inner field, m_s, is lumped at two nodes: one half, m_1, at the node adjacent to the pile, node 1, and the other one, m_2, at the node adjacent to the outer field, node 2 as shown in Fig. 1. If the material damping is to be added, a parallel dashpot may be considered with a constant c_m to be suitably chosen.

The equations of motion for the inner field expressing the equilibrium of masses m_1 and m_2 are

$$\begin{aligned} m_1\ddot{u}_1 + c_m(\dot{u}_1 - \dot{u}_2) + K_{nl}(u_1 - u_2) &= P_1 \\ m_2\ddot{u}_2 - c_m(\dot{u}_1 - \dot{u}_2) - K_{nl}(u_1 - u_2) &= P_2, \end{aligned} \tag{24}$$

where u_1 and u_2 are displacements of nodes 1 and 2, and P_1 is the force in the nonlinear spring which includes the confining pressure also, P_2 is the soil resistance at node 2; finally, c_m is the material damping in the inner field.

The equation of motion for the outer field may be written as

$$c\dot{u}_2 + K_l u = -P_2 + P, \tag{25}$$

where P is the interactive force transmitted through the soil from pile to pile. Introducing compatibility and equilibrium between the inner field and the outer field results in

$$\begin{Bmatrix} P_1 \\ 0 \end{Bmatrix} = \begin{bmatrix} A_m m_1 + A_c c_m + K_{nl} & -K_{nl} - A_c c_m \\ -K_{nl} - A_c c_m & K_{nl} + A_m m_2 + A_c c_t + K_l \end{bmatrix} \times \begin{Bmatrix} u_1 \\ u_2 \end{Bmatrix} + \begin{Bmatrix} \delta_1 \\ \delta_2 - P \end{Bmatrix}, \tag{26}$$

where $c_t = c + c_m$ is the total damping. From eqn (26) it can be deduced that

$$u_2 = \frac{K_{nl} + A_c c_m}{(K_{nl} + K_l + A_m m_2 + A_c c_t)} u_1 + \frac{P - \delta_2}{(K_{nl} + K_l + A_m m_2 + A_c c_t)} \tag{27}$$

$$P_1 = \left[K_{nl} + A_m m_1 + A_c c_m - \frac{(K_{nl} + A_c c_m)^2}{(K_{nl} + K_l + A_m m_2 + A_c c_t)}\right] w_1 - \frac{K_{nl}(P - \delta_2)}{(K_{nl} + K_l + A_m m_2 + A_c c_t)} + \delta_1, \tag{28}$$

where A_m and A_c are constants of numerical integration for inertia and damping, respectively. Finally

$$\delta_1 = K_{nl}^{i-1}(u_1 - u_2)^{i-1} + c_m(\dot{u}_1 - \dot{u}_2)^{i-1} + m_1\ddot{u}_1^{i-1} \tag{29}$$

$$\delta_2 = -K_{nl}^{i-1}(u_1 - u_2)^{i-1} - c_m(\dot{u}_1 - \dot{u}_2) + m_2\ddot{u}_2^{i-1} + K_l u_2^{i-1} + c\dot{u}_2^{i-1}. \tag{30}$$

Equations (24)–(30) are valid for soil nodes on both sides of the pile.

When the pile is moving away from the soil node, P_1 decreases until it reaches zero. If loading continues in the same direction, the resistance offered by that element will stay at zero (no tension is allowed) and the soil node on this side is disconnected from the pile node accommodating for the gap opening. On the other hand, when the pile is moving towards the soil node, P_1 increases until it reaches the maximum soil resistance and K_{nl} decreases until it reaches the value of zero; the near field spring on this side offers constant resistance to the pile motion. At this point, for some soil types, the ultimate static resistance of the soil may be reduced to display a post peak resistance as it has been observed for some soils such as dense sand and stiff clay. Reconnection of the soil–pile nodes occurs again when the pile returns to the displaced position of the soil node and continues to move in the direction of the soil node. The stiffness of the spring K_{nl} is assumed to be linear in the unloading phase.

Solution of equations of motion

For single piles and pile groups, the pile and soil displacements are evaluated in the time domain using the linear acceleration assumption and the Newmark β method for direct time integration of the equations of motion. The modified Newton–Raphson iteration scheme is used to derive and solve the governing equilibrium equations.

VALIDATION OF THE MODEL

The validity of the proposed nonlinear dynamic analysis is assessed through comparison with the results of some actual field tests as well as other analytical solutions in the literature.

Comparison with field tests

Full-scale field tests on single piles were conducted at the University of Houston. Piles were loaded with a static cyclic load (O'Niel & Dunnavant[14]) and a dynamic load (Blaney & O'Neil[15]). The soil profile at the site is shown in Fig. 6. Piles used in the tests are steel pipe piles with an outside diameter of 0·274 m and a wall thickness of 0·009 m. Figure 7 shows the piles and settings for both cyclic and dynamic tests. The proposed model was used to compute the response for both cases. The results from the analytical model and the field measurements are plotted in Fig. 8 for the cyclic load test and in Fig. 9 for the dynamic load test. The cyclic pile response was computed for a monotonically increasing load. The correlation between the computed and measured responses for both the cyclic and dynamic load test is very good and may be observed in Figs 8 and 9.

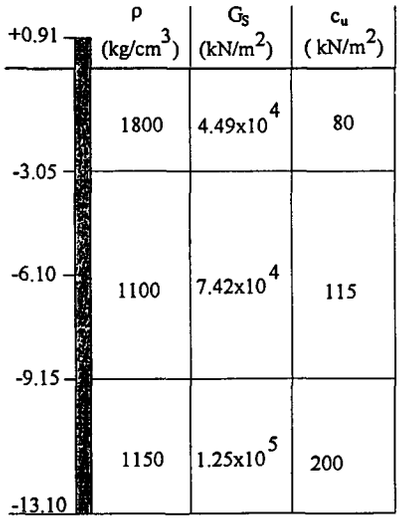

Fig. 6. Soil profile for University of Houston site.

Comparison with outer analytical approaches

To further examine the proposed model, the results obtained using the model are compared with those obtained using a more rigorous frequency domain solution due to Nogami.[16] The stiffness and damping parameters for a single pile and a group of two piles embedded in a homogeneous soil stratum underlain by a bed rock (Fig. 10) are computed using both approaches and plotted in Fig. 11 for the single pile case and Fig. 12 for the two-pile group. A very good agreement between the two results may be observed from the figures, especially for the single pile case.

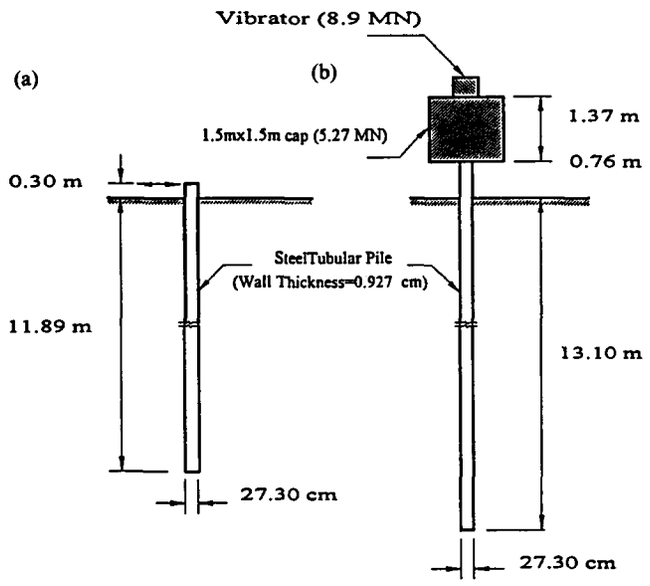

Fig. 7. Pile properties and test settings for (a) cyclic pile load test and (b) dynamic pile load test.

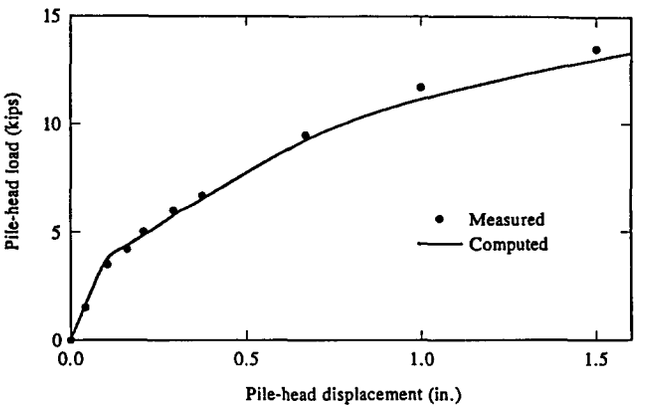

Fig. 8. Computed and measured cyclic pile response.

APPROXIMATE NONLINEAR ANALYSIS FOR PILE GROUP RESPONSE

The proposed analytical model may be applied to analyze the response of the entire pile group, accounting directly for the non-linearity and the interaction between all piles simultaneously. Alternatively, the superposition approach may be used to approximate the group response. To approximately account for group nonlinearity in the analysis, the equivalent linear single pile parameters, as well as interaction factors, have to be established depending on the P/P_U ratio, where P_U is the ultimate bearing capacity of the pile as defined by eqns (3)–(6) and P is the amplitude of the applied harmonic load at the pile head. Definitions for the single pile flexibilities, to be used to get the relevant stiffnesses, and interaction factors for the lateral response case are shown in Fig. 13.

Single piles

The stiffness and damping parameters of a single pile are computed for a steel pipe pile having an outer diameter of 1·45 m, a wall thickness of 0·05 m and a penetration depth of 50 m.

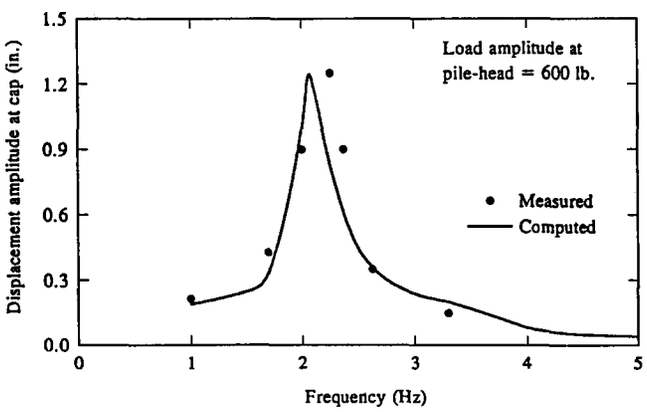

Fig. 9. Computed and measured dynamic pile response.

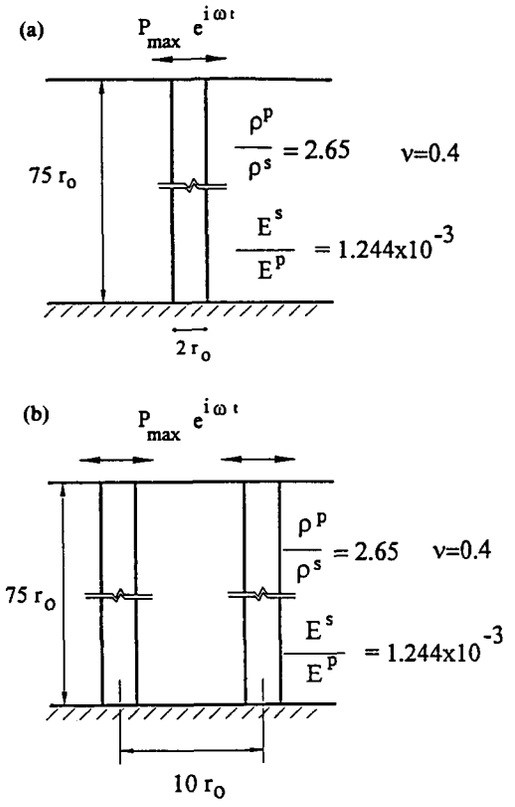

Fig. 10. Soil profile for the example used in the comparison with more rigorous frequency domain solution (a) single pile and (b) group of two identical piles.

Because of the coupling effect between the horizontal and rotational stiffnesses of the pile, the complex flexibilities for the horizontal, coupling, and rotational cases are calculated first and then the two by two complex flexibility matrix is inverted to obtain the complex stiffness matrix of the pile. The real part of the complex stiffness matrix represents the stiffness and the imaginary part represents the damping.

The flexibility terms are defined, as depicted in Fig. 13, using a unit horizontal load or a unit moment at the pile head and then calculating the corresponding deflections at the pile head. The horizontal flexibility is the

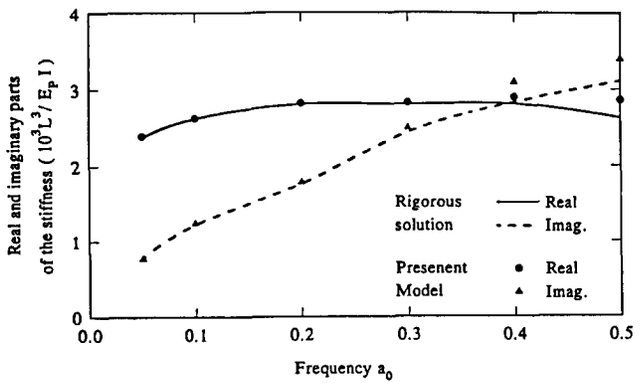

Fig. 11. Complex stiffness for a single pile.

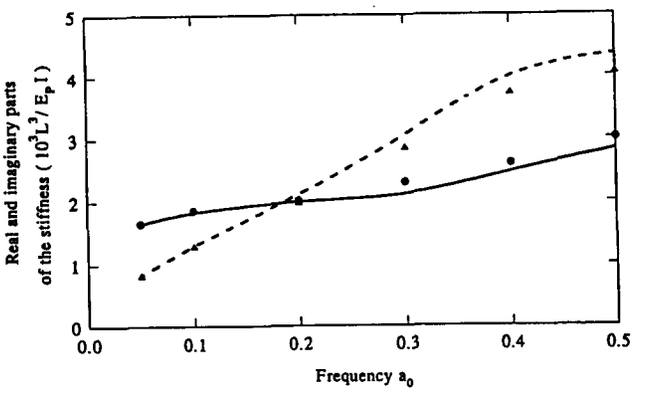

Fig. 12. Complex stiffness for two-pile group ($\theta = 0^0$).

horizontal translation due to horizontal load, the rotational flexibility is the rotation due to moment, and the coupling flexibility is the rotation due to a horizontal load or a horizontal translation due to moment. To compute these flexibilities approximately accounting for the nonlinearity, a harmonic load, or moment, with amplitude P, or M starting from zero is applied at the pile head and the response is then computed for a number of cycles until it stabilizes. The amplitude of the flexibility term, $|f_1|$, is approximated by the peak

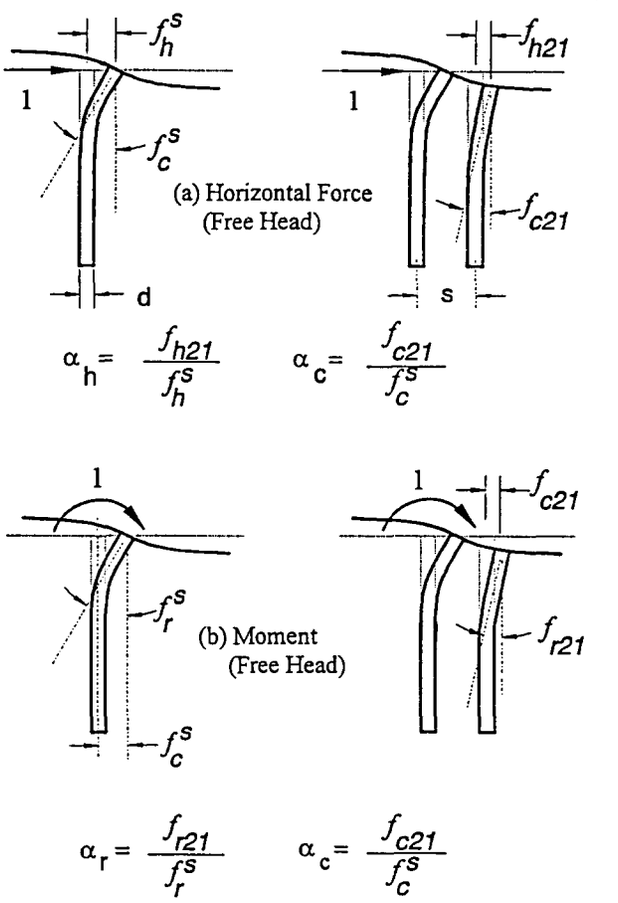

Fig. 13. Definition of single pile flexibility terms and interaction factors.

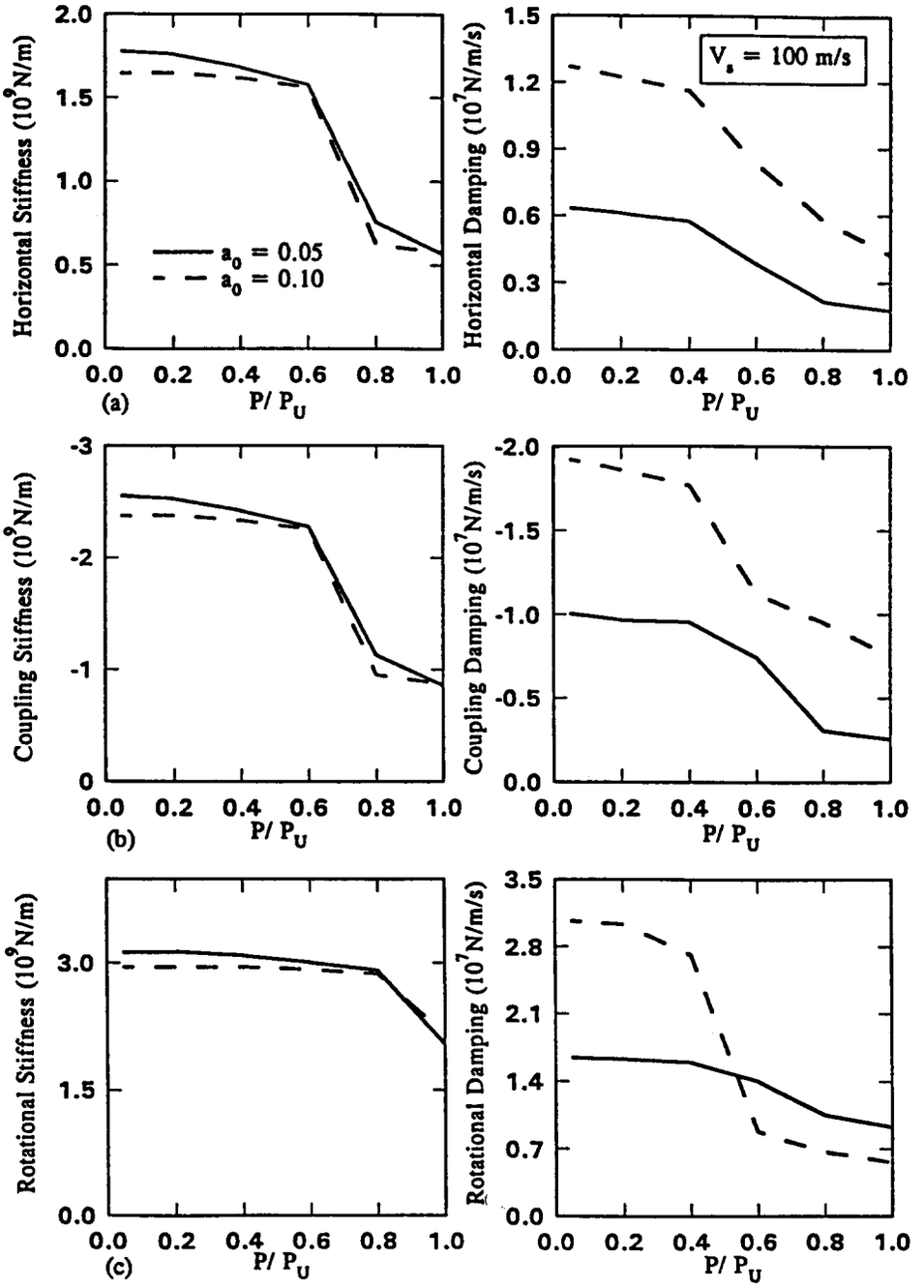

Fig. 14. Equivalent linear stiffness and damping for single piles in homogeneous soil profile (a) horizontal (b) coupling (c) rotational.

displacement divided by the amplitude of the applied load. The phase shift, ϕ_1, is approximated by the time lag between the peaks of both the displacement and load. The subscript 1 assumes different values for different flexibilities, i.e. h for horizontal, c for coupling and r for rotational. The figures displayed below show the variations of the equivalent linear stiffness and damping parameters for the horizontal, coupling and rotational cases with the loading ratio P/P_U.

Figure 14 shows the stiffness and damping constants for the pile embedded in a homogeneous soil medium whose $V_s = 100\,\mathrm{m\,s^{-1}}$ and excited with two different frequencies. The figure shows that as the loading ratio P/P_U increases, the horizontal and coupling stiffness constants decrease with mild slope until $P/P_U = 0{\cdot}6$; at this loading ratio the stiffness constants decrease dramatically until they reach one third of the linear case ($P/P_U = 0{\cdot}05$). The damping constants also display the same behavior, but they start decreasing at lower loading ratios. The decrease in the rotational stiffness is negligible up to $P/P_U = 0{\cdot}8$, but the decrease in the damping is significant even at lower P/P_U ratios, especially for the higher frequency. Stronger nonlinear effects are observed for nonhomogeneous soil profiles and stiffer soils.

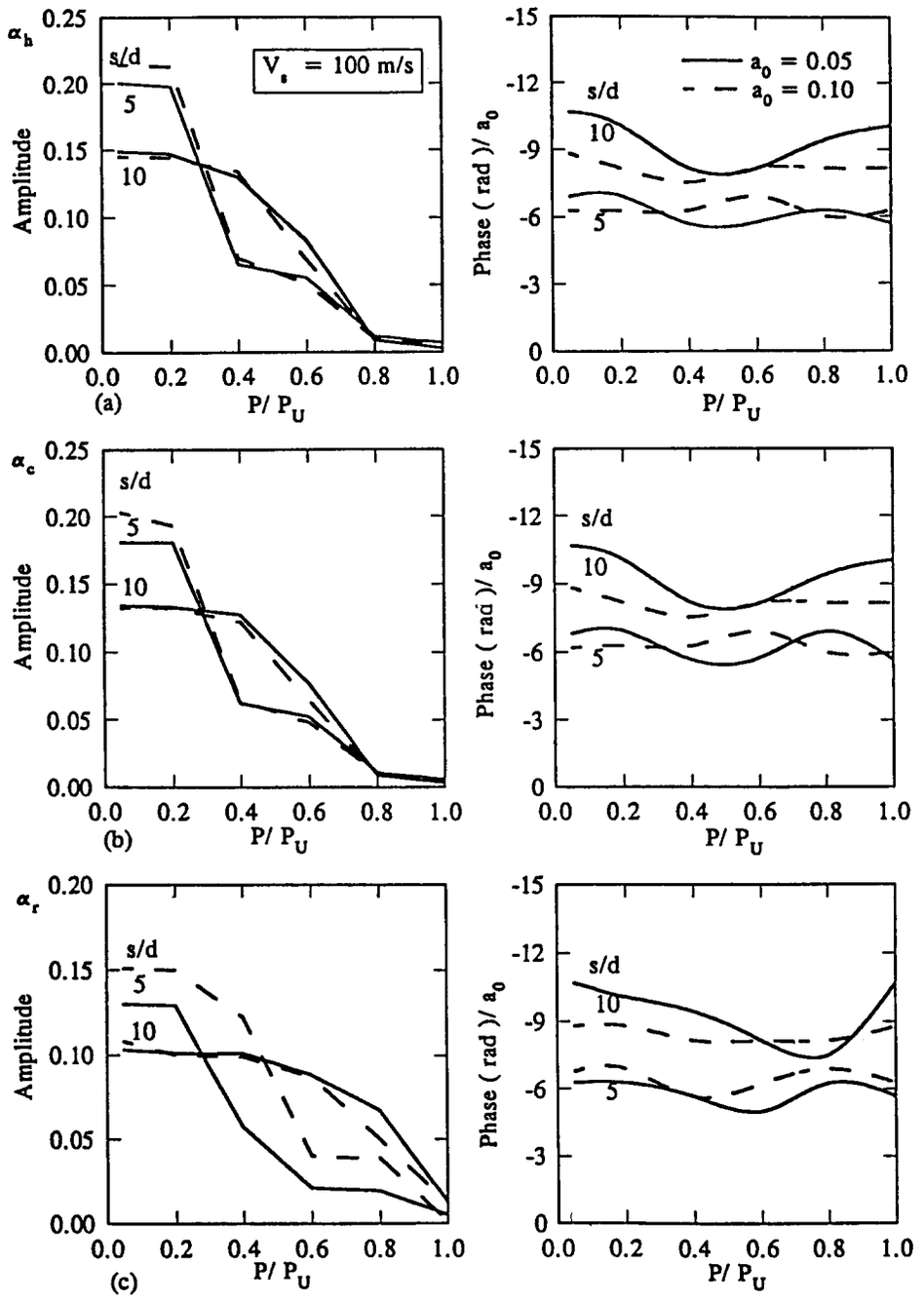

Fig. 15. Dynamic interaction factors for approximate nonlinear analysis for piles in homogeneous soil ($\theta = 0^0$) (a) horizontal (b) coupling (c) rotational.

Interaction factors

The interaction coefficients are needed to perform the group analysis using the superposition approach. To account approximately for the nonlinear effects in the lateral group analysis, the interaction factors should be established taking the load level and nonlinear conditions into consideration.

The equivalent linear interaction factor is defined as the displacement of a load-free pile normalized by the displacement of the loaded contiguous pile when no other piles are present (Fig. 13). To establish the equivalent linear interaction factors, two loading cases are considered separately: a pile loaded individually and a group of two identical piles with only one of them loaded. The resulting deflection at the pile head is

$$u_{lm}(t) = |u_{lm}| e^{i\phi_{lm}}. \tag{31}$$

In eqn (31), $|u_l|$ is the amplitude, either in horizontal translation or rotation, approximated by the peak deflection, and ϕ_l is the phase shift, approximated by the time

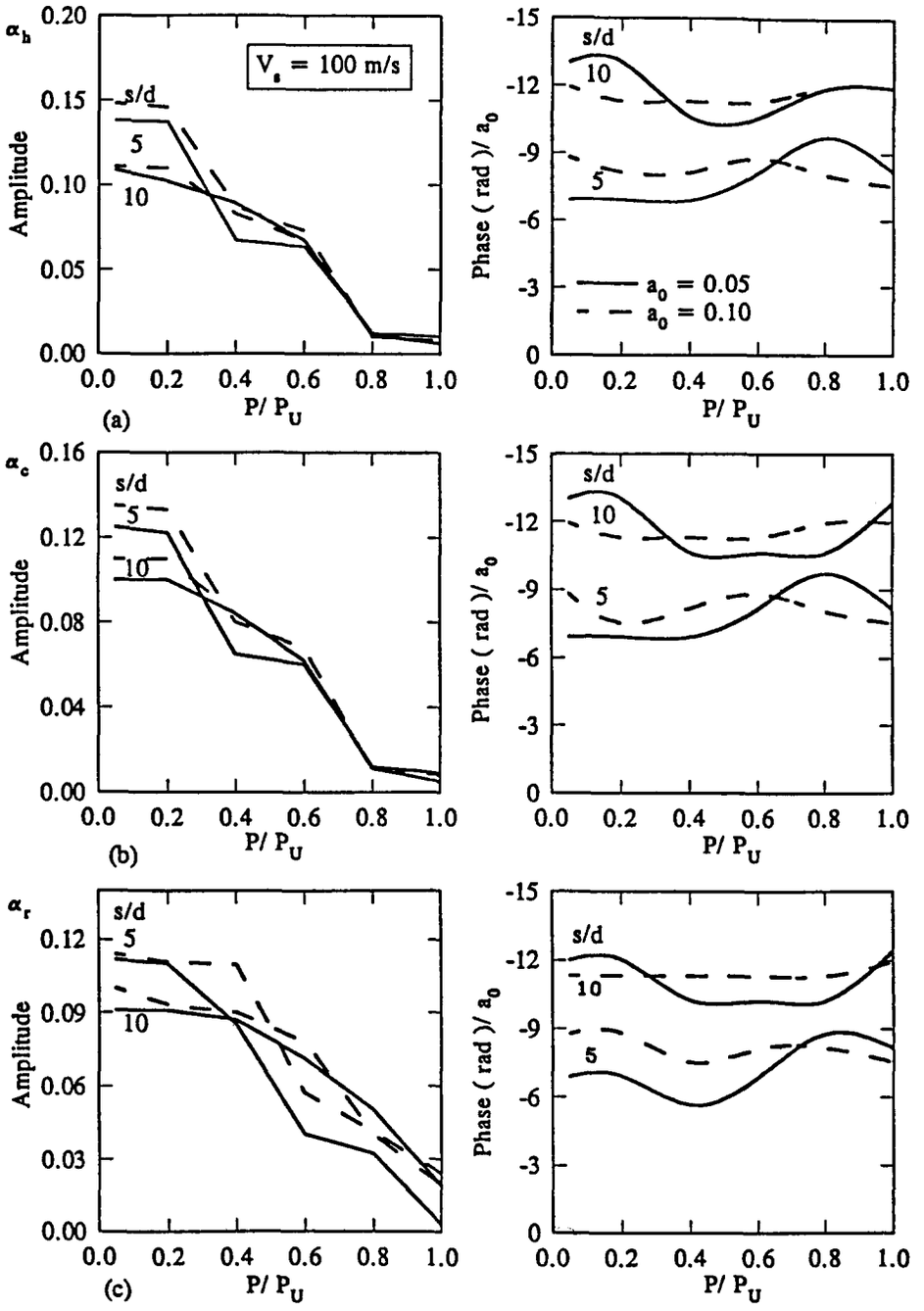

Fig. 16. Dynamic interaction factors for approximate nonlinear analysis for piles in homogeneous soil ($\theta = 90^0$) (a) horizontal (b) coupling (c) rotational.

lag between the peaks of both the deflection and force. The subscript m takes the values 0 for the case of single pile loading and 1 for the load-free pile in the second case of loading. The loading starts from zero and the amplitude and phase shift are established after five loading cycles. The response was found to stabilize almost completely after this number of cycles. The interaction factor is defined as

$$\alpha_l = \frac{u_{l1}(t)}{u_{l0}(t)}. \tag{32}$$

The dynamic interaction factor is a complex quantity which can be described either by its real and imaginary parts, α_1 and α_2, or in terms of its absolute value, $|\alpha|$, and phase shift ϕ. Thus the interaction factor, α, may be written as

$$\alpha = \alpha_1 + i\alpha_2 = |\alpha| e^{i\phi}. \tag{33}$$

The amplitude, $|\alpha_1|$, and the phase shift, ϕ_1, of the interaction factor resulting from eqn (32) may be

approximated by

$$|\alpha_1| = \frac{|u_{11}|}{|u_{10}|} \qquad (34)$$
$$\phi_1 = \phi_{11} - \phi_{10}.$$

Figures 15 and 16 show the interaction factors for a pile embedded in homogeneous soil with shear wave velocity $V_s = 100\,\mathrm{m\,s^{-1}}$, for two pile to pile spacing to diameter ratios, $s/d = 5$ and 10, and two different frequencies for the angles $\theta = 0^0$ and 90^0, respectively. It may be observed from the figures that a dramatic decrease occurs in the amplitude as P/P_U starts increasing, for the horizontal, coupling and rotational cases. The phase shift oscillates, yet still could be considered constant.

Similar nonlinearity effects were found to take place in parabolic and linear soil media with different shear wave velocities.

CONCLUSIONS

(1) The lateral dynamic response computed using the proposed model compares favourably with field-measured data as well as the more rigorous frequency domain approach. The model uses only conventional soil mechanics parameters or parameters directly correlated to them.

(2) Single pile stiffness and damping parameters, as well as interaction between the piles, are greatly affected by the level of loading. Such an effect should be included in the analysis of the dynamic lateral response of pile groups, particularly for strongly nonhomogeneous soil profiles and limit state considerations.

(3) The effect of nonlinearity is that it reduces single pile and pile group stiffness as well as damping. Also, nonlinearity reduces the amplitude of interaction factors between piles, while the phase shift oscillates, but still may be considered constant. These effects are more pronounced for stiffer soils or softer piles, such as those typical of offshore structures.

(4) Finally, the model facilitates direct analysis of a pile group lateral response to dynamic loading with little computing effort and allows the generation of interaction factors for different loading ratios, different pile spacing to diameter ratios and different soil profiles. For a basic range of parameters, the nonlinear interaction factors are provided.

ACKNOWLEDGMENTS

This research was supported by a grant-in-aid of research from the Natural Sciences and Engineering Research Council of Canada.

REFERENCES

1. Blaney, G. W., Kausel, E. & Roesset, J. M., Dynamic stiffness of piles, *Proc. 2nd Int. Conf. on Numerical Methods in Geomechanics*, Vol. 2, 1976, pp. 1001–1012.
2. Kuhlemeyer, R. L., Static and dynamic laterally loaded floating piles, *J. Geotech. Eng. Div. ASCE*, 1979, **105,** 325–330.
3. Banerjee, P. K., Analysis of axially and laterally loaded pile groups. In *'Developments in Soil Mechanics'*, ed. Scott, C. R., Chap. 9. Applied Science Publications, London, 1978, pp. 317–346.
4. Kaynia, A. M. & Kausel, E., Dynamic behavior of pile groups, *Proc. 2nd Int. Conf. on Numerical Methods in Offshore Piling*, I.C.E., April, 1982, pp. 509–532.
5. Matlock, H., Foo, S. H. C. & Bryant, L. M., Simulation of lateral pile behavior under earthquake motion, *Speciality Conf. on Earthquake Engineering and Soil Dynamics*, Pasadena, June, 1978, pp. 600–619.
6. Nogami, T. & Konagai, K., Time domain flexural response of dynamically loaded single piles, *J. Engng Mech. Div. ASCE*, 1988, **114,** 1512–1525.
7. Novak, M., Nogami, T. & Aboul-Ella, F., Dynamic soil reactions for plane strain case, *J. Engng Mech. Div. ASCE*, 1978, **104,** 953–959.
8. Novak, M. & Sheta, M., Approximate approach to contact problems of piles, *Proc. Geotechnical Engineering Division, ASCE, National Convention, Dynamic Response of Pile Foundations: Analytical Aspects*, Florida, 30 October, 1980, pp. 53–79.
9. American Petroleum Institute, *Recommended Practice for Planning, Designing and Constructing Fixed Offshore Platforms, API Recommended Practice 2A* (RP 2A), 19th Edn, Washington, D.C., 1991.
10. Poulos, H. G., Behaviour of laterally loaded piles: I — single piles, *J. Soil Mech. Foundations Div.* ASCE, 1971, **97,** SM5, Proceedings Paper 8902, 711–732.
11. El Sharnouby, B. & Novak, M., Static and low frequency response of pile groups, *Can. Geotech. J.*, 1985, **22,** 79–84.
12. Gazetas, G. & Dobry, R., Horizontal response of piles in layered soils, *J. Geotech. Engng Div. ASCE*, 1984, **110,** 20–40.
13. Makris, N. and Gazetas, G., Dynamic pile-soil-pile interaction. Part II: lateral and seismic response, *J. Earthquake Engng Struct. Dyn.*, 1992, **21,** 145–162.
14. O'Neil, M. W. & Dunnavant, T. W., A study of the effects of seals, velocity and cyclic degradability on laterally loaded single piles in overconsolidated clay, Research Rep. UHCE84-7, Department of Civil Engineering, University of Houston, 1984.
15. Blaney, G. W. & O'Neil, M. W., Lateral response of a single pile in overconsolidated clay to relatively low frequency pile-head load and harmonic ground surface loads, Research Rep. UHCE83-19, Department of Civil Engineering, University of Houston, 1983.
16. Nogami, T., *Dynamic Stiffness and Damping of Pile Groups in Inhomogeneous soil*, ASCE Special Technical Publications on *Dynamic Response of Pile Foundations: Analytical Aspects*, 1980, pp. 31–52.
17. Nogami, T., Konagai, K. & Otani, J., Nonlinear time domain numerical model for pile group under transient dynamic forces, *Proc. 2nd Int. Conf. on Recent Advances in Geotechnical Earthquake Engineering and Soil Dynamics*, St. Louis, Missory, Paper no. 5.51, 1991.
18. Dobry, R. & Gazetas, G., Simple method for dynamic stiffness and damping of floating pile groups, *Geotechnique*, 1988, **38,** 557–574.